Cartilage Thickness and Bone Shape Variations as a Function of Sex, Height, Body Mass, and Age in Adult Knees.

Marco Tien-Yueh Schneider (msch153@aucklanduni.ac.nz)
Auckland Bioengineering Institute
Nynke Rooks
Auckland Bioengineering Institute
Thor Besier
Auckland Bioengineering Institute

Research Article

Keywords: Knee morphology, Cartilage thickness, Thickness distribution, Bone shape, Statistical Shape Model

Posted Date: October 29th, 2021

DOI: https://doi.org/10.21203/rs.3.rs-900199/v1

Title: Cartilage thickness and bone shape variations as a function of sex, height, body mass, and age in adult knees.

Authors and affiliations:

Marco Tien-Yueh Schneider*
- Auckland Bioengineering Institute, The University of Auckland, Auckland, New Zealand

Nynke Rooks
- Auckland Bioengineering Institute, The University of Auckland, Auckland, New Zealand

Thor Besier*
- Auckland Bioengineering Institute, The University of Auckland, Auckland, New Zealand
- Department of Engineering Science, The University of Auckland, Auckland, New Zealand

Co-author emails:
Nynke Rooks
– nroo469@aucklanduni.ac.nz

Thor Besier
– t.besier@auckland.ac.nz

Corresponding author:
Marco Tien-Yueh Schneider
Address: Auckland Bioengineering Institute, University of Auckland, Level 6, 70 Symonds Street, Auckland 1010, New Zealand
Telephone: +64 9 373 7599
Email: msch153@aucklanduni.ac.nz

Keywords:
Knee morphology
Cartilage thickness
Thickness distribution
Bone shape
Statistical Shape Model

Word Count:
Introduction - 475
Methods - 683
Results - 572
Discussion - 1155
Total - 2885

Abstract (348 words)

The functional relationship between bone and cartilage is modulated by mechanical factors. Scarce data exist on the relationship between bone shape and the spatial distribution of cartilage thickness. This study has three aims: first, to characterise the coupled variation in knee bone morphology and cartilage thickness distributions in knees with healthy cartilage. The second aim was to investigate this relationship as a function of sex, height, body mass, and age. The third aim was to characterise the morphological differences between males and females. MR images of 51 adult knees (28.4±4.1 years) were obtained from a previous study and used to train a statistical shape model of the femur, tibia, and patella and their cartilages. Five linear regression models were fitted to characterise morphology as a function of sex, height, body mass, and age. A logistic regression classifier was fitted to characterise morphological differences between males and females, and 10-fold cross-validation was performed to evaluate the models' performance. Our results showed that cartilage thickness and its distribution was coupled to bone morphology, including both size (mode 1) and shape variations (mode 2 onwards). The first three shape modes captured over 90% of the variance and described the overall size, diaphysis size, femoral shaft angle, and corresponding changes to the spatial distribution of the cartilages. These modes were sex-linked ($p < .0001$, $p < .05$, $p < .01$, for modes 1, 2, and 3 respectively) and could classify sex with an accuracy of 94.1% (95% CI [83.8%, 98.8%]). Height was a predictor of joint size ($p <. 0001$) and diaphysis size ($p < .05$). Body mass was a predictor of joint size ($p < .1$) and femoral shaft angle ($p < .1$). Age was not correlated with any of the modes. This study demonstrated the coupled relationship between bone and cartilage, showing that cartilage is thicker with increased bone size, diaphysis size, and decreased femoral shaft angle. Our findings show that sexual dimorphism is strong in these first three modes, and that bone shape and cartilage thickness at the joint are strongly correlated with height but weakly correlated with mass.

Introduction (475 words)

The functional relationship between bone and cartilage is complex and is modulated by mechanical factors introduced by loading and motion [1]. Mature cartilage has a location-dependent histomorphology that is developed in response to its specific loading history [1]. The mechanical stresses and strains experienced by the cartilage over time influence the morphology and material properties of the tissue. Conversely, the morphology of bone and cartilage influence the instantaneous stresses and strains experienced in the joint [2]. Bone size and shape can affect the contact area and the lines of action crossing the joint [3], while cartilage thickness influences the mechanical properties of cartilage [4] and the stresses and strains experienced in the tissue [2,5,6]. Characterising the relationship between bone and cartilage morphology *in vivo* is important to understand the knee joint's functional anatomy and pathology.

Knee bone morphology has been characterised as a function of sex [7,8], osteoarthritis (OA) [9-12], and knee ligament injury [13]. Studies have also quantified cartilage thickness across individuals [5,14-16] and found that cartilage is generally thicker where cartilage stresses are high [6,17]. Males appear to have greater volume of knee cartilage compared to females [18,19], and cartilage morphology is in part mediated by size and mass [15,17,18]. However, these studies have analysed cartilage and bone morphology in isolation or have simplified cartilage morphology to a singular value (such as cartilage volume or mean thickness), and thus, do not capture the complexity and nuance of the coupled variation in cartilage thickness distribution and bone morphology in three dimensions. This information has important implications for understanding the onset of osteoarthritis, the development of surrogate and predictive models, and the design of implants.

Statistical shape modelling (SSM) characterises complex 3D morphologies by decomposing shape features into a set of statistically significant principal components that describe the main variations in the population [20,21]. The shape features can be extended to include scalar field values (such as cartilage thickness, and bone mineral density) to explore shape-field relationships. The principal components, or modes, can then be used to visualize these variations, and correlated to parameters such as patient demographics to quantitatively examine differences between cohorts [10,22-24]. To the best of our knowledge, statistical shape models have not been employed to characterise the coupled morphological variations of adult knee bones and their cartilage thickness distribution in relation to subject demographics.

The purpose of this study was firstly to develop a statistical shape model of the femur, tibia, and patella and their cartilages to characterise and describe the coupled variation in bone morphology and cartilage thickness in a cohort of 51 knees with healthy cartilage. Secondly, we investigated the effects of sex, height, body mass, and age, on the morphology of the knee joint bones and cartilage using linear regression. Lastly, we characterised the morphological differences in coupled bone shape and cartilage thickness distribution between males and females.

Methods (683 words)

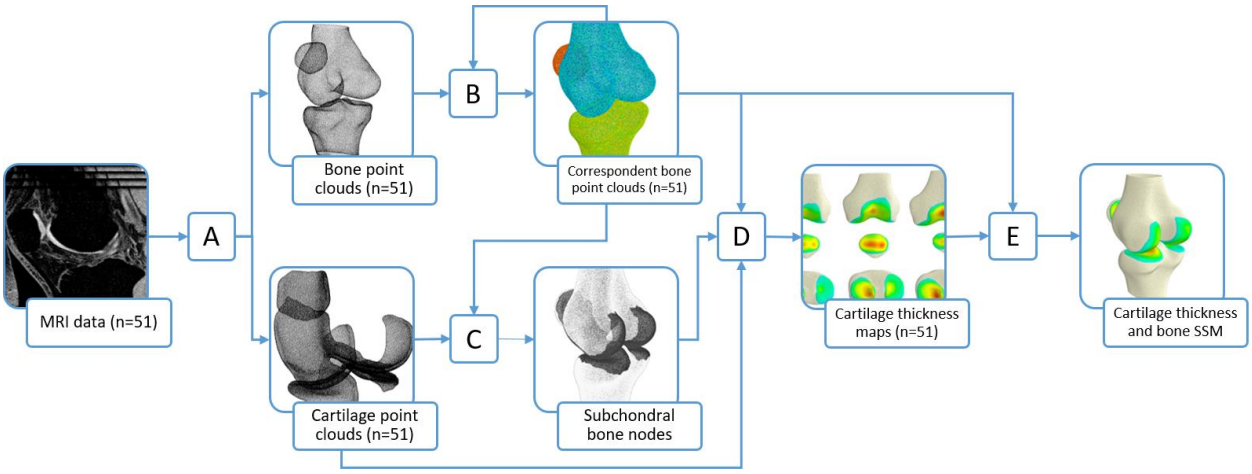

Figure 1. Schematic of workflow to generate cartilage thickness field and bone shape model. MR images (n=51) of the knee were segmented, processed in MAPClient, and resampled (A) to produce bone and cartilage point clouds. Parametric bone point clouds were obtained via an iterative fitting process (B). Subchondral bone node numbers on these correspondent point clouds were found by combining node numbers obtained from all subjects using a closest-point algorithm (C). Cartilage thickness maps were calculated (D) by computing the magnitude of the projection of the closest articular cartilage point to the normal vector of each subchondral bone node. Principal component analysis (E) was performed on features consisting of the corresponding nodal coordinates of the bone and cartilage thickness per subchondral node to produce a statistical model of the cartilage thickness and bone shape.

MR images (n=51) of adult knees (28.4 ± 4.1 years, Table 1) were obtained from an ongoing study on patellofemoral pain[16,25,26], where all participants were screened by a radiologist to ensure they had no cartilage damage or degenerative changes. All participants were advised on all aspects of the study and analysis of data before informed consent was obtained. Permission was obtained to analyse the data in this study. Ethics approval for this study (Reference #3346) was granted by the Stanford University Institutional Review Board, and the procedures followed were in accordance with the ethical standards of the responsible committee on human experimentation (institutional and national) and with the Helsinki Declaration of 1975, as revised in 2000. All methods were carried out in accordance with relevant guidelines and regulations. The bones, including the femur, patella, tibia, and their corresponding cartilages were manually

segmented in Stradwin [27] to produce triangulated surface meshes and point clouds (Figure 1 A). To correct for the varying field of view (FOV) in the imaging data, MAPClient [28] was used to fit an existing statistical shape model (SSM) to the femurs and tibias (Figure 1 A). The femurs were then cropped at a height equal to the epicondylar width and the tibias were cropped at a height equal to the width of the tibial plateau.

Table 1. Subject demographics.

	Number	Age (years)	Height (cm)	Body Mass (kg)
Total	51	28.4 ± 4.1	172.0 ± 8.5	65.6 ± 10.2
Females	30	28.2 ± 4.6	167.5 ± 5.9	60.6 ± 7.7
Males	21	29.3 ± 3.7	178.4 ± 7.4	72.7 ± 9.0

A published method [10,22,24] was adapted to maximise nodal correspondence in the bone point clouds and create a training set of parametric point clouds (Figure 1 B).

Bone point clouds were resampled in Meshlab [29] to generate template point clouds with mean nearest neighbour distance of 0.5 mm and mesh density of ~2.6 points per mm^2 for the femur, tibia, and patella (Figure 1A). The template point clouds were iteratively fitted to the training set data via a series of coarse to fine fits using adaptive radial basis function fitting to generate a training set of maximally correspondent points [30]. Rigid alignment of the training set data to the templates was achieved by minimising the least squared distances of corresponding nodes. Principal component analysis (PCA) was performed on the correspondent nodes to generate an intermediate statistical shape model of the bones [31]. This process was repeated with the shape model as the template until the correspondent RMS error between the point cloud in the current and previous iteration was less than 0.01mm.

The cartilage point clouds were resampled (Figure 1 A) to a density of ~16 points per mm^2, resulting in ~200,000 points for the femoral cartilage, ~50,000 points for the patellar cartilage,

and ~50,000 points each for the lateral and medial tibial cartilages. The cartilage point clouds for each subject in the training set were overlaid with their corresponding parametric bone point clouds and a closest point algorithm was used to identify bone nodes that were subchondral (Figure 1 C). These bone nodes were combined to produce a list of subchondral bone nodes shared by the training set.

The cartilage thickness was then calculated for each subchondral bone node (Figure 1 D) [32]. The closest articular cartilage point to the normal of each subchondral bone node was projected onto the normal vector. The magnitude from the subchondral bone node to this projection was calculated to obtain the thickness at that subchondral bone node. This calculation was performed on the femur, tibia, and patella for all subjects in the training set (n=51) to obtain correspondent maps of cartilage thickness.

Correspondent nodes and cartilage thickness at each node were then analysed using PCA. A 2D matrix was constructed with n-rows (n=51 independent observations) and m-columns of features, consisting of nodal coordinates and thickness values. PCA was performed on this matrix to produce a statistical shape and field model (SSFM) of bone shape and cartilage thickness (Figure 1 E).

To address the first aim, the model was used to reconstruct figures of the mean and standard deviations of the first 3 principal components to characterise the main modes of variation in the bone and cartilage of the knee. To address the second aim, linear regression was used to investigate the influence of sex, height, body mass, and age on the SSFM scores of the first n modes, such that the cumulative variation captured was over 95%.

To address the final aim, a logistic regression model [33] was trained on the scores of the SSFM to characterise the coupled morphological differences in bone shape and cartilage thickness

distribution between males and females. Principal components were added in a stepwise fashion until no more statistically significant improvement of the fit of the model was observed. 10-fold stratified cross-validation was performed to evaluate the models performance.

Results (572 words)

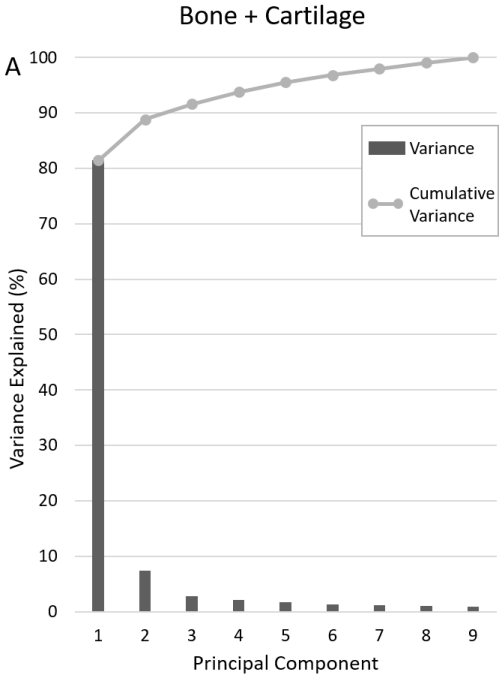

Figure 2. Variation and cumulative variation represented by principal component number for the statistical bone shape and cartilage thickness model.

The first five principal components (or modes) of the SSFM of bone shape and cartilage thickness captured over 95% of the variation in the morphology in the training set (Figure 2). The regions with the thickest cartilage in the femur were located in the trochlear groove, the femoral condyles, and along the medial condyle (Figure 3). In the tibia, the thickest cartilage was found in the lateral tibial plateau. In the patella, the thickest cartilage was generally located centrally with some variations where the distribution bifurcated across the patella's vertical ridge.

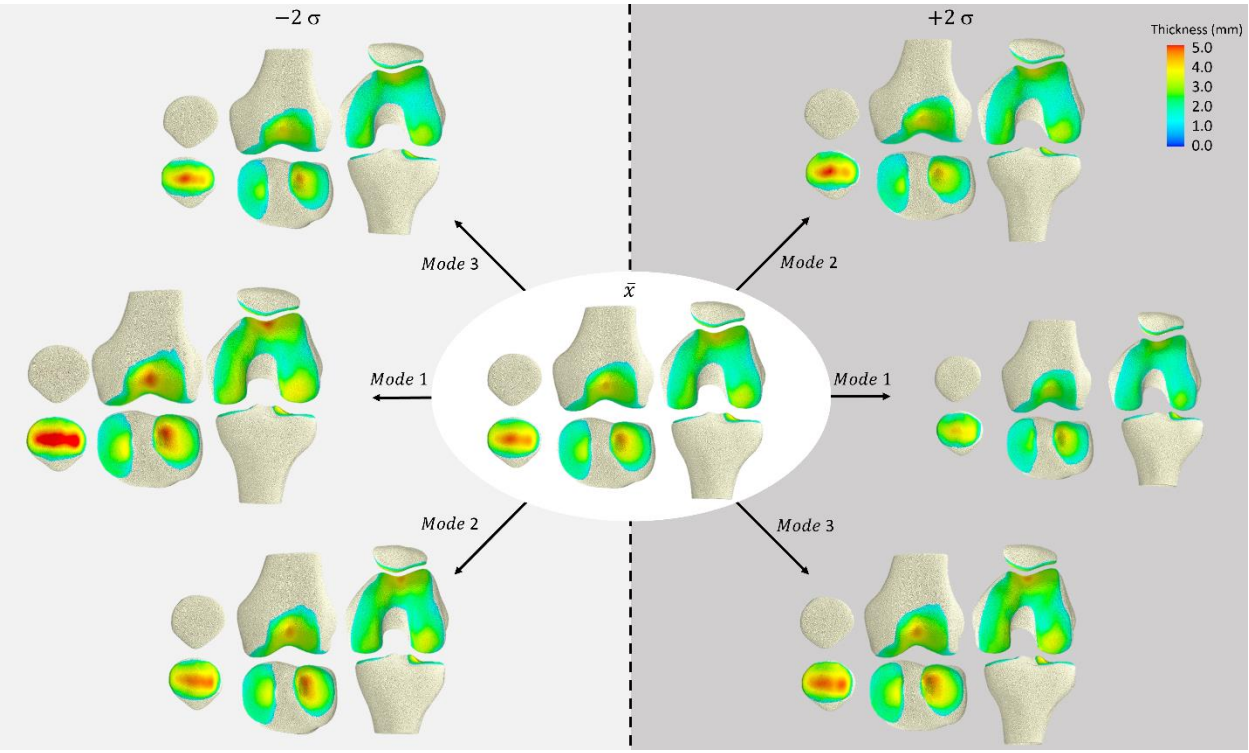

Figure 3. The first three modes of coupled variation of the statistical bone shape and cartilage thickness model of the knee bones and cartilage.

The first mode qualitatively explained differences in the overall size of the knee bones as well as the overall thickness of the cartilage (Figure 3). From this model, we observed that bone size was coupled to cartilage thickness, with larger bones having thicker cartilage.

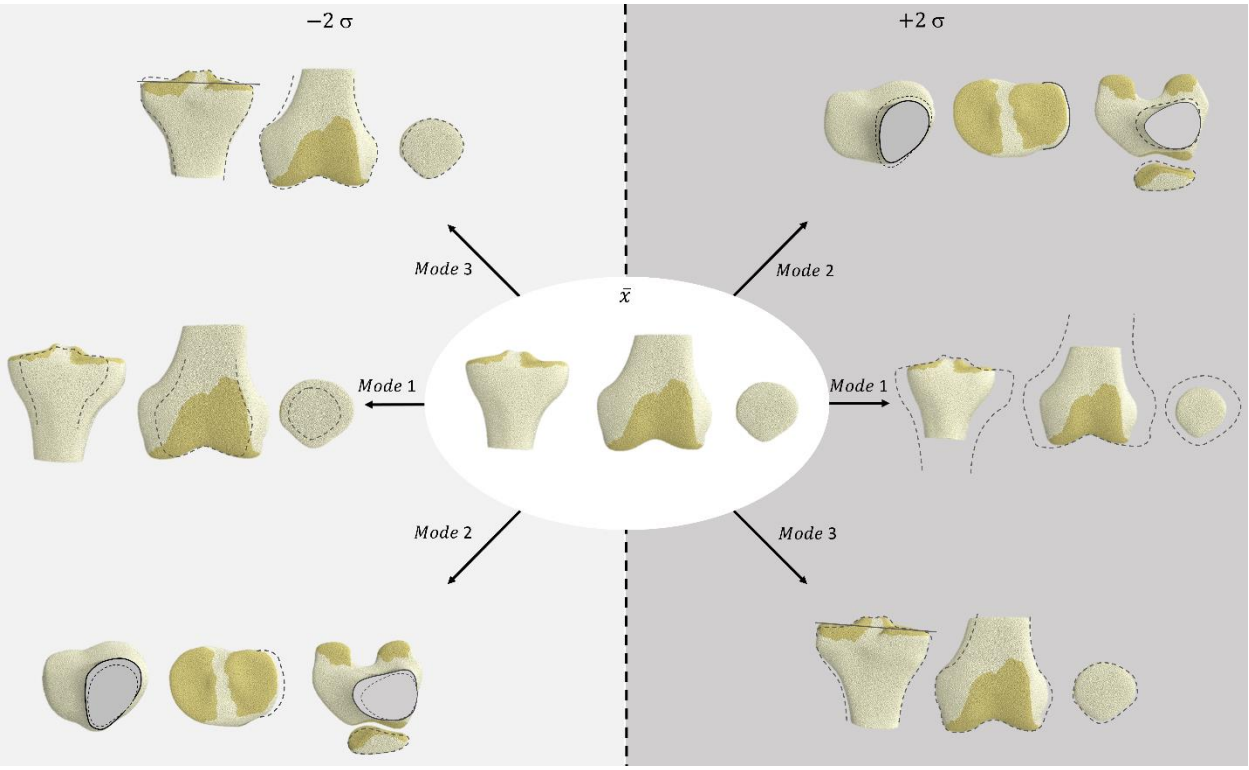

Figure 4. The first three modes of bone shape variation of the statistical bone shape and cartilage thickness model of the knee bones and cartilage.

The second mode described coupled changes associated with aspect ratio of the bones and cartilage. In the bones (Figure 4), we observed coupled changes in the size of the diaphysis relative to the width of the epiphyses in both the femur and tibia. In the tibia, we also saw a widening of the tibial plateau with decreased diaphysis size. Additionally, this mode captured changes in the anterior-posterior thickness of the patella, which was lower with decreased diaphysis size. In the cartilage, we observed a number of coupled changes across the bones (Figure 5), including thinning of cartilage in both the femur and tibia with decreased diaphysis size, and a proximal-distal shift in the location of the thickest cartilage in both the patella and trochlea cartilage. Furthermore, thinning of the trochlear cartilage on the femur was coupled with thicker patellar cartilage.

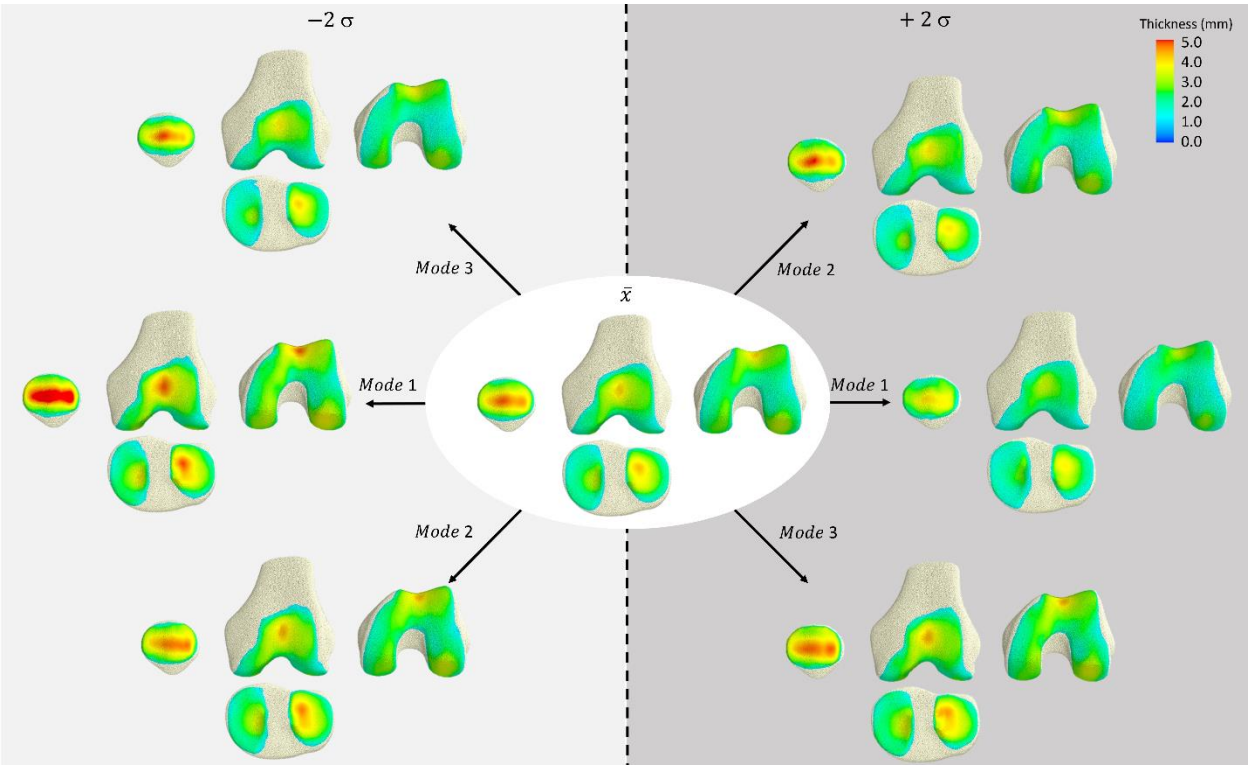

Figure 5. The first three modes of cartilage thickness variation visualised on the mean bone of the statistical bone shape and cartilage thickness model of the knee bones and cartilage.

In the bone, the third mode describes changes to the angle of the femoral shaft axis to the epicondylar axis (femoral shaft angle) and the mediolateral tilt of the tibial plateau. A larger femoral shaft angle was accompanied with a flatter tibial plateau (Figure 4). In addition, a ridge located on the medial side of the patella was observed to become more prominent with this increased angle. This larger femoral shaft angle was accompanied with thinner cartilage throughout and a more inferiorly located cartilage boundary in the trochlear (Figure 5). We also observed a narrowing of the medial and lateral boundaries of the trochlear cartilage (Figure 3).

Table 2. Standardised coefficients (beta) of linear regression for modes in the SSFM.

Mode	**1**	**2**	**3**	4	5
Sex	**-0.396*** **	**0.400** **	**-0.518*** **	0.0300	0.112
Height	**-0.419*** **	**-0.572** **	0.210	-0.200	-0.0958
Mass	**-0.197***	0.271	**-0.380***	0.0234	0.283
Age	-0.0334	-0.132	0.0628	0.223	-0.171
R^2	0.813	0.167	0.222	0.0688	0.088

*, **, *** indicates significance at the 90%, 95%, and 99% level, respectively.

Linear regression models were fitted for the first five modes of the SSFM (Table 2. The first mode (size) was strongly influenced by sex ($p < .0001$) and height ($p < .0001$), and weakly influenced by body mass ($p < .1$). The second mode was influenced by sex ($p < .05$) and height ($p < .05$). The third mode was influenced by sex ($p < .01$) and weakly influenced by body mass ($p < .1$). No other modes were influenced by sex, height, body mass, or age.

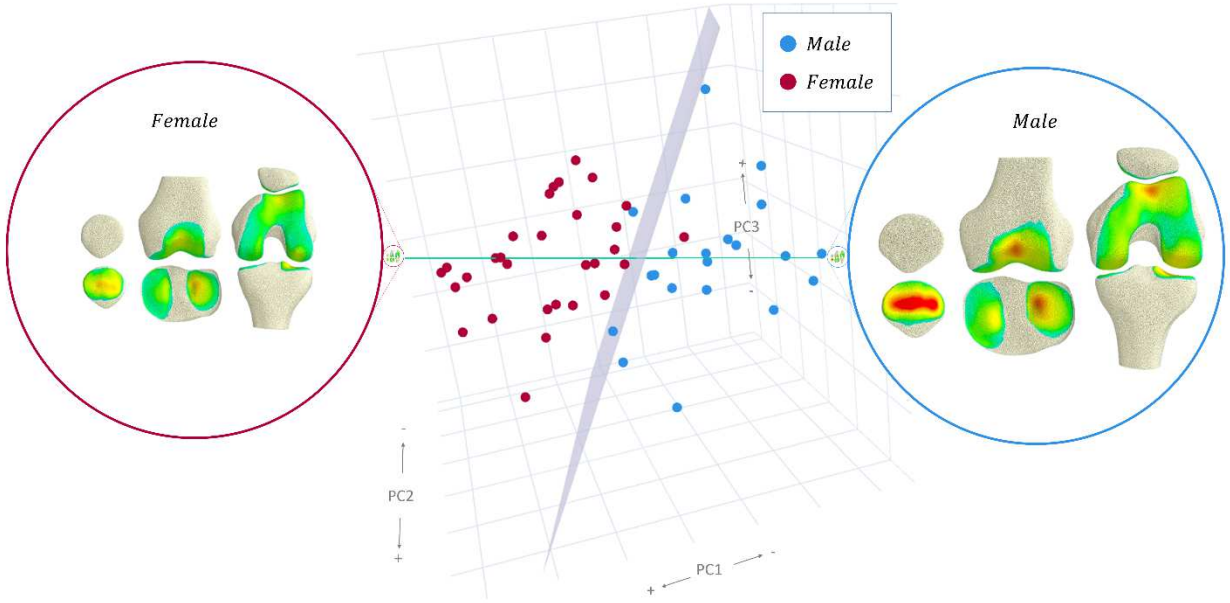

Fig. 6. 3D scatter of the first three principal components of the training set by sex, showing the decision boundary plane (grey) of the logistic regression model, and, a vector (green) that passes through the average male and female knee.

The logistic regression model trained on the first three principal components (Figure 6) of the SSFM scores characterised the morphology of the bone and cartilage between males and females to an accuracy of 96.1% within the training set. Cross-validation of this model yielded a classification accuracy of 94.1% (95% CI [83.8%, 98.8%]) and an area under the curve (AUC) of 95.8%. The decision boundary (Figure 6), shows that females had generally smaller bones (positive PC1) accompanied with lower aspect ratios (negative PC2), steeper mediolateral tibial tilt and lower femoral shaft angle (positive PC3).

Discussion (1155 words)

The purpose of this study was to develop a statistical shape and field model of the femur, tibia, patella, and their cartilages to characterise the coupled variation in bone morphology and cartilage thickness in a cohort of healthy knees. The bone shape and cartilage field model captured over 95% of the variance with the first five modes. This model was interrogated to explore the effects of sex, height, body mass, and age, on the morphology of the bones and cartilage thickness distribution, and finally used to characterise the morphological differences between males and females. We found that sex and height strongly influenced knee joint morphology, while body mass influenced knee joint morphology to a lesser extent. Finally, age did not influence morphology in this adult cohort.

Our results show that cartilage thickness and its distribution is coupled to bone morphology, including both size (mode 1) and shape variations (mode 2 onwards).
The greatest influence on the overall cartilage thickness was bone size, where larger bones displayed thicker cartilage (Figure 3, mode 1). Although this seems intuitive, studies across

species have shown that cartilage thickness does not necessarily scale with size. For example, the cartilage in the larger stifle joint in horses (equivalent to human knee) is thinner than knee cartilage in the smaller human knee [34,35]. Within the lower limb joints of humans, Shepherd and Seedhom [36] hypothesised that cartilage thickness is a function of joint congruency, due to the hip and ankle having thinner cartilage than the knee in their sample of 11 cadavers. This is believed to be related to how much stress the cartilage needs to bear [6,17]. We expect an increase in body mass with bone size to result in increased stress that requires thicker cartilage to bear. Studies have also reported a correlation between anthropomorphic measurements such as height and mass to mean cartilage thickness [15,17,36], implying a relationship between bone size, stress, and cartilage thickness. Our results confirm this finding in a larger sample (n=51), where height and mass were both correlated to increased overall cartilage thickness (mode 1). Similar to previous studies, mass also only described some of the variability in cartilage thickness [15,17,36]. This seems intuitive as mass is not directly related to muscle and joint contact force, or the load history during growth and adolescence where the bone and cartilage is undergoing a modelling process [37]. Indeed, the joint moments produced during locomotion are scaled relative to height x mass. Interestingly, the same height x mass relationship accounts for the muscle volumes in the lower limb [38].

Our model showed that cartilage thickness is coupled to bone shape variations. Knees with smaller diaphyses (mode 2) possessed thinner cartilage overall and the location of the thickest cartilage in the patella and trochlea shifted proximally, whereas knees with larger diaphyses possessed thicker cartilage. Increased diaphysis size increases the bone section modulus which typically results from increased load experienced during growth and development [39]. This increased load bearing may explain why this feature is accompanied with thicker cartilage. Interestingly, thinner cartilage in the trochlear groove was also accompanied with thicker cartilage in the patella. Assuming that thinner cartilage occurs where congruence is high, this

mode may describe the amount of congruence mismatch between the tibiofemoral joint and the patellofemoral joint.

The mediolateral slope of the tibial plateau and the angle of the femoral shaft axis are also coupled (mode 3) where a larger angle is accompanied with thinner cartilage. Recent studies have reported that a high Q-angle (similar to the femoral shaft axis angle) is negatively correlated with cartilage thickness [40], especially in the lateral compartment [41]. Kusiak and Kawczyński [41] hypothesised that this is due to increased compression imposed by the patellar cartilage on this condyle. This explanation seems insufficient, as the cartilage is thicker along the inner region of the medial condyle (Figure 3) than any region on the lateral condyle [6]. Without knowledge of the muscle force distribution on the patella and the contact mechanics of the patellofemoral articulation, it is difficult to draw any conclusions regarding patellofemoral joint mechanobiology. Further modelling work might uncover these form-function relationships and sex differences.

Sexual dimorphism was present in the first three modes of the model (Figure 6). Size (mode 1) and shape (mode 2 and 3) of both the bone and cartilage are important for classifying sex. On average, this means females present a smaller joint with thinner cartilage, larger angle between the femoral shaft axis and the epicondylar axis, and smaller diaphysis compared to males. This is somewhat expected and conforms with previous studies that have demonstrated sexual dimorphism in bone morphology [10]. Prior studies have reported differences in cartilage volume between males and females, where males had larger cartilage volumes than females [16-19,42]. Our results add to these previous findings by giving further clarity as to how the spatial distribution of the cartilage thickness varies in the population along with variations to bone morphology. We expect further modelling work to reveal how cartilage stress is maintained across different bone and cartilage morphologies.

There are many implications of this work. It is important to consider both the cartilage morphology as well as the bone morphology as they both influence the mechanics. This is particularly important when considering joint contact models as the cartilage thickness influences the mechanical response of the cartilage and the internal stresses experienced by the tissue. In implant design, the articulating geometry needs to be considered, not just the subchondral bone. This method can be extended to include an OA cohort to compare the coupled changes in bone and cartilage morphology as a function of osteoarthritis progression.

There are several limitations in this work that should be acknowledged. Firstly, the conclusions drawn in this paper are limited to knees with healthy cartilage, as determined by a musculoskeletal radiologist as part of the inclusion criteria from the original experimental study [16]. Our methodology normalised for bone orientation, a factor that may influence the interaction between bones and hence the cartilage thickness. As the scope of this study was to characterise the coupled variation in bone morphology and cartilage thickness, we did not investigate how these relationships are affected when normalised for bone size or maximum cartilage thickness. Lastly, as with any investigation of bone and cartilage morphology using medical imaging data, our results are subject to manual segmentation errors which are typically < 0.5mm for knee joint structures [32].

In conclusion, we have characterised and described the coupled variation in bone morphology and cartilage thickness in a cohort of 51 adult knees. We observed that cartilage is thicker with increased bone size, diaphysis size, and decreased femoral shaft angle. Sexual dimorphism was present in these three modes which could be used to understand the dimorphism that exists in OA, knee ligament injuries, and patellofemoral pain. Lastly, we found that bone

morphology and cartilage thickness were strongly correlated with height but weakly correlated with body mass.

Acknowledgements

This work was supported by the Auckland Bioengineering Institute and by the National Institutes of Health (Award numbers 1R01EB024573-01 and 1R01EB005790-01). We thank Christine Draper and Garry Gold for help with data collection. The content is solely the responsibility of the authors and does not necessarily represent the official views of the Auckland Bioengineering Institute or the National Institutes of Health.

Author Contributions

All authors have made significant contribution to the conception and design of the study, acquisition of data, and interpretation of data. Development of the computational models and, drafting of the paper were performed by M.T.S. T.B. and N.R. contributed to critical revision of the paper and approved the final version of the manuscript to be published.

Data availability statement

The data that support the findings of this study are openly available in SimTK.org Anatomical Knee at https://simtk.org/projects/anatomicalknee

Competing Interests Statement

The author(s) declare no competing interests.

References

1 Carter, D. R. *et al.* The mechanobiology of articular cartilage development and degeneration. *Clinical Orthopaedics and Related Research®* **427**, S69-S77 (2004).

2 Anderson, A. E., Ellis, B. J., Maas, S. A. & Weiss, J. A. Effects of idealized joint geometry on finite element predictions of cartilage contact stresses in the hip. *Journal of Biomechanics* **43**, 1351-1357, doi:https://doi-org.ezproxy.auckland.ac.nz/10.1016/j.jbiomech.2010.01.010 (2010).

3 Arnold, A. S. & Delp, S. L. Rotational moment arms of the medial hamstrings and adductors vary with femoral geometry and limb position: implications for the treatment of internally rotated gait. *Journal of Biomechanics* **34**, 437-447 (2001).

4 Thambyah, A., Nather, A. & Goh, J. Mechanical properties of articular cartilage covered by the meniscus. *Osteoarthritis and Cartilage* **14**, 580-588 (2006).

5 Ateshian, G. A., Soslowsky, L. J. & Mow, V. C. Quantitation of articular surface topography and cartilage thickness in knee joints using stereophotogrammetry. *Journal of Biomechanics* **24**, 761-776, doi:https://doi-org.ezproxy.auckland.ac.nz/10.1016/0021-9290(91)90340-S (1991).

6 Li, G. *et al.* The cartilage thickness distribution in the tibiofemoral joint and its correlation with cartilage-to-cartilage contact. *Clinical Biomechanics* **20**, 736-744, doi:https://doi-org.ezproxy.auckland.ac.nz/10.1016/j.clinbiomech.2005.04.001 (2005).

7 Zhang, J., Fernandez, J., Hislop-Jambrich, J. & Besier, T. F. Lower limb estimation from sparse landmarks using an articulated shape model. *Journal of biomechanics* **49**, 3875-3881 (2016).

8 Zhang, J. & Besier, T. F. Accuracy of femur reconstruction from sparse geometric data using a statistical shape model. *Computer methods in biomechanics and biomedical engineering* **20**, 566-576 (2017).

9 Bredbenner, T. L. *et al.* Statistical shape modeling describes variation in tibia and femur surface geometry between Control and Incidence groups from the Osteoarthritis Initiative database. *Journal of Biomechanics* **43**, 1780-1786, doi:https://doi-org.ezproxy.auckland.ac.nz/10.1016/j.jbiomech.2010.02.015 (2010).

10 Lynch, J. T. *et al.* Statistical shape modelling reveals large and distinct subchondral bony differences in osteoarthritic knees. *Journal of Biomechanics* **93**, 177-184, doi:https://doi-org.ezproxy.auckland.ac.nz/10.1016/j.jbiomech.2019.07.003 (2019).

11 Felson, D. T. *et al.* The incidence and natural history of knee osteoarthritis in the elderly, the framingham osteoarthritis study. *Arthritis & Rheumatism* **38**, 1500-1505 (1995).

12 Wise, B. L. *et al.* Bone shape mediates the relationship between sex and incident knee osteoarthritis. *BMC musculoskeletal disorders* **19**, 331 (2018).

13 Pedoia, V. *et al.* Three-dimensional MRI-based statistical shape model and application to a cohort of knees with acute ACL injury. *Osteoarthritis and Cartilage* **23**, 1695-1703, doi:https://doi-org.ezproxy.auckland.ac.nz/10.1016/j.joca.2015.05.027 (2015).

14 Cohen, Z. A. *et al.* Knee cartilage topography, thickness, and contact areas from MRI: in-vitro calibration and in-vivo measurements. *Osteoarthritis and Cartilage* **7**, 95-109, doi:https://doi-org.ezproxy.auckland.ac.nz/10.1053/joca.1998.0165 (1999).

15 Eckstein, F., Winzheimer, M., Hohe, J., Englmeier, K. H. & Reiser, M. Interindividual variability and correlation among morphological parameters of knee joint cartilage plates: analysis with three-dimensional MR imaging. *Osteoarthritis and Cartilage* **9**, 101-111, doi:https://doi-org.ezproxy.auckland.ac.nz/10.1053/joca.2000.0365 (2001).

16 Draper, C. *et al.* Is cartilage thickness different in young subjects with and without patellofemoral pain? *Osteoarthritis and cartilage* **14**, 931-937 (2006).

17 Connolly, A., FitzPatrick, D., Moulton, J., Lee, J. & Lerner, A. Tibiofemoral cartilage thickness distribution and its correlation with anthropometric variables. *Proc Inst Mech Eng H* **222**, 29-39, doi:10.1243/09544119JEIM306; 23 10.1243/09544119JEIM306 (2008).
18 Ding, C., Cicuttini, F., Scott, F., Glisson, M. & Jones, G. Sex differences in knee cartilage volume in adults: role of body and bone size, age and physical activity. *Rheumatology* **42**, 1317-1323 (2003).
19 Faber, S. C. *et al.* Gender differences in knee joint cartilage thickness, volume and articular surface areas: assessment with quantitative three-dimensional MR imaging. *Skeletal radiology* **30**, 144-150 (2001).
20 Cootes, T. F., Cooper, D. H., Taylor, C. J. & Graham, J. Trainable method of parametric shape description. *Image and Vision Computing* **10**, 289-294 (1992).
21 Dryden, I. L. & Mardia, K. V. (New York, NY: John Wiley & Sons, Ltd, 1998).
22 Schneider, M. *et al.* Men and women have similarly shaped carpometacarpal joint bones. *Journal of biomechanics* **48**, 3420-3426 (2015).
23 Schneider, M. T. *et al.* Trapeziometacarpal joint contact varies between men and women during three isometric functional tasks. *Medical engineering & physics* **50**, 43-49 (2017).
24 Schneider, M. *et al.* Early morphologic changes in trapeziometacarpal joint bones with osteoarthritis. *Osteoarthritis and cartilage* **26**, 1338-1344 (2018).
25 Pal, S. *et al.* Patellofemoral cartilage stresses are most sensitive to variations in vastus medialis muscle forces. *Computer methods in biomechanics and biomedical engineering* **22**, 206-216 (2019).
26 Besier, T. F. *et al.* The role of cartilage stress in patellofemoral pain. *Medicine and science in sports and exercise* **47**, 2416 (2015).
27 Treece, G., Prager, R. & Gee, A.
28 Zhang, J. *et al.* in *International Symposium on Biomedical Simulation.* 182-192 (Springer).
29 Corsini, M., Cignoni, P. & Scopigno, R. Efficient and flexible sampling with blue noise properties of triangular meshes. *IEEE transactions on visualization and computer graphics* **18**, 914-924 (2012).
30 Zhang, J., Ackland, D. & Fernandez, J. Point-cloud registration using adaptive radial basis functions. *Computer methods in biomechanics and biomedical engineering* **21**, 498-502 (2018).
31 Zhang, J., Hislop-Jambrich, J. & Besier, T. F. Predictive statistical models of baseline variations in 3-D femoral cortex morphology. *Medical engineering & physics* **38**, 450-457 (2016).
32 Rooks, N. *et al.* A Method to Compare Heterogeneous Types of Bone and Cartilage Meshes. *Journal of Biomechanical Engineering* (2021).
33 Demšar, J. *et al.* Orange: data mining toolbox in Python. *the Journal of machine Learning research* **14**, 2349-2353 (2013).
34 Frisbie, D. D., Cross, M. W. & McIlwraith, C. W. A comparative study of articular cartilage thickness in the stifle of animal species used in human pre-clinical studies compared to articular cartilage thickness in the human knee. *Veterinary and comparative orthopaedics and traumatology* **19**, 142-146 (2006).
35 Firth, E. C. The response of bone, articular cartilage and tendon to exercise in the horse. *Journal of anatomy* **208**, 513-526, doi:https://doi-org.ezproxy.auckland.ac.nz/10.1111/j.1469-7580.2006.00547.x (2006).
36 Shepherd, D. E. T. & Seedhom, B. B. Thickness of human articular cartilage in joints of the lower limb. *Annals of the Rheumatic Diseases* **58**, 27-34 (1999).

37 Jones, G. *et al.* Knee articular cartilage development in children: a longitudinal study of the effect of sex, growth, body composition, and physical activity. *Pediatric research* **54**, 230-236 (2003).
38 Handsfield, G. G., Meyer, C. H., Hart, J. M., Abel, M. F. & Blemker, S. S. Relationships of 35 lower limb muscles to height and body mass quantified using MRI. *Journal of biomechanics* **47**, 631-638 (2014).
39 Ruff, C. Growth in bone strength, body size, and muscle size in a juvenile longitudinal sample. *Bone* **33**, 317-329, doi:https://doi-org.ezproxy.auckland.ac.nz/10.1016/S8756-3282(03)00161-3 (2003).
40 Ayşe Aydemir, E., Hamarat, H. & Musmul, A. Relationship between Q-angle and articular cartilage in female patients with symptomatic knee osteoarthritis: ultrasonographic and radiologic evaluation. *Archives of rheumatology* **32**, 347 (2017).
41 Kusiak, M. & Kawczyński, A. Ultrasonographic assessment of articular cartilage of the femoral condyle in patients with an increased Q-angle. *Journal of ultrasonography* **18**, 181 (2018).
42 Cicuttini, F. *et al.* Gender differences in knee cartilage volume as measured by magnetic resonance imaging. *Osteoarthritis and Cartilage* **7**, 265-271, doi:https://doi-org.ezproxy.auckland.ac.nz/10.1053/joca.1998.0200 (1999).

[dataset] Schneider MT, Rooks N, Besier TF. (2021) Anatomical Knee.

https://simtk.org/projects/anatomicalknee